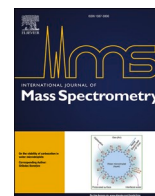


<https://doi.org/10.1016/j.ijms.2023.117128>

Access to this work was provided by the University of Maryland, Baltimore County (UMBC) ScholarWorks@UMBC digital repository on the Maryland Shared Open Access (MD-SOAR) platform.

Please provide feedback

Please support the ScholarWorks@UMBC repository by emailing scholarworks-group@umbc.edu and telling us what having access to this work means to you and why it's important to you. Thank you.



Analysis of intramolecular carbon isotope distributions in alanine by electrospray ionization Orbitrap mass spectrometry

Gabriella M. Weiss^{a,b,*}, Alex L. Sessions^a, Maxime Julien^{c,d}, Timothy Csernica^e, Keita Yamada^d, Alexis Gilbert^{d,f}, Katherine H. Freeman^b, John M. Eiler^a

^a Division of Geological and Planetary Sciences, California Institute of Technology, Pasadena, CA, 91125, USA

^b Department of Geosciences, The Pennsylvania State University, University Park, PA, 16803, USA

^c GFZ German Research Centre for Geosciences - Helmholtz Centre Potsdam, Organic Geochemistry, Potsdam, Germany

^d Department of Chemical Science and Engineering, Tokyo Institute of Technology, Yokohama, 226-8503, Kanagawa, Japan

^e Division of Chemistry and Chemical Engineering, California Institute of Technology, Pasadena, CA, 91125, USA

^f Earth-Life Science Institute, Tokyo Institute of Technology, Meguro, 152-8550, Tokyo, Japan

ARTICLE INFO

Keywords:

Electrospray ionization
Orbitrap
Position-specific isotope analysis
Carbon isotopes
Amino acids
Isotope ratio mass spectrometry

ABSTRACT

The ability to detect intramolecular isotopic differences within a single molecule can answer questions about molecule synthesis and alteration across numerous scientific fields. Until recently, intramolecular (i.e., position-specific isotope analysis, PSIA) isotope measurements were laborious, requiring large amounts of analyte or specialized instrumentation. Orbitrap™ mass spectrometers are capable of fragmenting molecules and have the high mass resolution needed to constrain position-specific isotopic differences among the resulting fragment ions. Orbitrap mass spectrometers with electrospray ionization accurately measured the molecular average isotope composition of acetate, nitrate, sulfate, phosphate, and the amino acid methionine, as well as the position-specific isotopic structure of methionine. Here, we document the ability of this method to measure the position-specific carbon isotope structure of the amino acid alanine. Data include measurements of ¹³C-enriched materials to assign specific atoms in fragments to the original molecular structure and detect any recombination of atoms in resultant fragments. We further demonstrate high-precision intramolecular isotope analyses for standards with independently determined position-specific carbon isotope compositions. Isotope data from ESI-Orbitrap-MS agrees with values obtained using gas source isotope ratio mass spectrometry, giving further confidence to this novel approach to PSIA. The carbon isotope analyses by Orbitrap-MS were rapid and required ~5 µg of analyte to obtain both molecular average and position-specific values in triplicate with precision ≤1%.

Author contributions

Gabriella M. Weiss: Methodology, ESI-Orbitrap-MS and EA-IRMS analysis and data processing, writing, visualization, project administration.

Alex L. Sessions: Methodology, funding, writing.

Maxime Julien: Methodology, sample preparation, EA-IRMS, GC-C-IRMS and GC-py-GC-C-IRMS analysis, writing.

Timothy Csernica: Methodology, ESI-Orbitrap-MS analysis and data processing, writing.

Alexis Gilbert: Methodology, writing, project administration.

Keita Yamada: EA-IRMS analysis, acetaldehyde isotopic standard preparation.

Katherine H. Freeman: Project administration, funding, writing.

John M. Eiler: Methodology, writing, project administration.

Abbreviations: EA, elemental analyzer; ESI, electrospray ionization; GC, gas chromatography; HPLC, high performance liquid chromatography; IRMS, isotope ratio mass spectrometry; Isotopologue, molecules with the same chemical formula but different isotope composition; M+1, isotopic species with an isotopic substitution having a cardinal mass increase of 1 relative to the abundant isotope; MA, molecular average (resulting from compound-specific isotope analysis or CSIA); MS, mass spectrometry; PSIA, position-specific isotope analysis; Py, pyrolysis; SPME, solid phase microextraction.

* Corresponding author. Division of Geological and Planetary Sciences, California Institute of Technology, Pasadena, CA, 91125, USA.

E-mail address: gabriella.weiss@nasa.gov (G.M. Weiss).

¹ Now at Astrochemistry Department, NASA Goddard Space Flight Center, Greenbelt, MD, USA & Center for Space Sciences and Technology, University of Maryland Baltimore County, Baltimore, MD, USA.

<https://doi.org/10.1016/j.ijms.2023.117128>

Received 23 May 2023; Received in revised form 18 August 2023; Accepted 20 August 2023

Available online 25 August 2023

1387-3806/© 2023 Elsevier B.V. All rights reserved.

1. Introduction

Stable isotope analysis of light elements (C, H, O, N, S) is commonly used to trace biogeochemical cycles and study the origin and fate of natural compounds [1]. A molecule's isotopic composition can record its source substrates, the (bio)chemical pathways of its synthesis, fluxes associated with its formation, and mechanisms and fluxes associated with its destruction. Many of these processes are sensitive to environmental variables such as temperature or CO₂ partial pressure.

Most isotopic analyses are performed using isotope ratio mass spectrometry (IRMS). This approach combusts or reduces target molecules into analyzable gases (e.g., CO₂ for carbon or N₂ for nitrogen). Isotope analyses of these small gasses averages isotopic information from all positions within an analyte and yields a single value that is the molecular average (the ratio of ¹³C/¹²C in a sample relative to ¹³C/¹²C in a standard; here written $\delta^{13}\text{C}_{\text{MA}}$ in the case of carbon). IRMS methods can include on-line coupling with liquid or gas chromatography (HPLC and GC, respectively), which enable isotopic analysis of individual compounds within complex mixtures, yielding molecular average values to be recovered for each compound (compound-specific isotope analysis, CSIA).

Molecular average isotope compositions, however, obscure information potentially recorded by the rare isotope distribution within the molecule. A variety of chemical and physical processes can lead to significant differences in isotopic composition between non-equivalent atomic sites. In addition, the MA approach obscures proportions of multiply substituted isotopologues, also referred to as “clumped” rare isotope species. To access the isotope composition at individual atomic positions within a molecule (i.e., position-specific isotope analysis, PSIA), several methods have been developed (Table 1), including chemical or enzymatic degradation of a target compound followed by isotope analysis of generated products that sample subsets of the analyte's molecular structure [2–4], on-line thermal degradation (pyrolysis) coupled with IRMS [5–8], direct PSIA by nuclear magnetic resonance (NMR) [9–12], and fragmentation in a high-resolution mass spectrometer [13–15].

In the present study, we use the latter method of PSIA by Electrospray Ionization Orbitrap™ Mass Spectrometry (ESI-Orbitrap-MS) to characterize the intramolecular carbon isotope variation of the amino acid alanine. We examined alanine that was artificially ¹³C-enriched at individual carbon positions to understand fragmentation and recombination within the mass spectrometer. Understanding any recombination that occurs and the potential alterations to the isotopic composition of a given molecule is an essential step in exploring the use of Orbitrap mass spectrometry for making position-specific isotope measurements. Additionally, it is important to establish which atomic positions in the whole molecule correspond to positions within the fragment ions. We use ¹³C-enrichments to understand these processes. Having established

this, we then measured a variety of standards having approximately natural isotope abundances to test how the accuracy and precision of ESI-Orbitrap-MS measurements compare to established IRMS analyses.

High resolution mass spectrometry (HRMS) allows quantification of intramolecular variation without extensive sample preparation, large sample size requirements, or specialized, non-commercial instrumentation. Molecules are introduced for analysis intact and without conversion to simple gasses (e.g., as for traditional IRMS). In this study, derivatization of compounds was not required. For natural mixtures, off-line or on-line separation is sometimes necessary, but not used in this study. Provided the ion fragment masses differ from each other and contaminant (i.e., non-analyte) ions, Orbitrap mass spectrometry's relatively high mass resolution (often in the range 10^{5–6}, M/ΔM) can distinguish sample and contaminant ions. In such cases, signatures of individual compounds can be isolated from mixtures without extensive preparation. HRMS also permits isotope ratios of multiple elements to be determined within a single acquisition (e.g., Refs. [14,16]).

Both HPLC and GC can be coupled to Orbitrap mass spectrometers to provide on-line separation for complex mixtures and enable PSIA [13, 17–20]. In fact, these instruments are widely used for proteomics and metabolomics workflows that separate and identify compounds in complex mixtures (e.g., Ref. [21]). Molecular average isotope analysis by ESI-Orbitrap-MS has been demonstrated for acetate [16], nitrate [22, 23], sulfate and phosphate [22], and the amino acid methionine [14]. Intramolecular differences were noted for a suite of methionine samples that are linked to the molecule's origins [14], demonstrating the potential for using ESI-Orbitrap-MS for PSIA. However, PSIA measurements using mass spectrometric fragmentation must include standards with clear position-specific isotope enrichments to document the relationship between fragment ions and molecular atom positions, and to identify any scrambling of atomic positions that can occur within the instrument which could obscure the apparent isotopic contrast between positions. Isotope labels are used to determine presence or absence of recombination of atomic sites during analysis. It was noted that no recombination occurs with amino acid fragments analyzed by GC-pyrolysis-GC-C-IRMS [6], but this has not been tested for ESI-Orbitrap-MS until now.

Amino acids are important target analytes for PSIA. They are ubiquitous in nature, essential to all living systems, and are known to have intramolecular isotopic differences related to their synthesis [2]. They are the building blocks of proteins and present in all life on Earth, produced abiotically via several synthesis reactions (e.g. Ref. [24], and found on meteorites [18,25,26]). Their carbon skeletons collectively sample a broad swath of central metabolic pathways, providing excellent potential for reconstructing metabolisms.

The first application of position-specific isotope methods focused on amino acids produced by photosynthetic organisms [2]. This first study proposed that for 12 different amino acids, the carboxyl (C-1) position is

Table 1

Details about different methods of position-specific isotope analysis (PSIA). Strengths and weaknesses of each type of PSIA are presented. It is important to note that individual analytical goals and available resources are the overall determining factor for which method is best for a given project.

Method	Measured species	Sensitivity (nmol)	Strengths	Weaknesses	Select References
Chemical or enzymatic degradation + IRMS	Conversion of analyte to CO ₂	100s	Uses established IRMS methods, ability to constrain all positions	Many steps, requires derivatization, large sample size, long analysis times	[2–4]
Pyrolysis + IRMS	Conversion of analyte to CO ₂	100s	Uses established IRMS methods, ability to constrain all positions	Many steps, requires derivatization, large sample size, long analysis times	[5–7]; Dias et al. (2022)
NMR	Intact molecule	50,000–300,000	Ability to constrain all positions, non-destructive, derivatization not required	large sample size (100s of mmol)	[9,10]; Rasmussen and Hoffman (2020)
Orbitrap-MS	Molecular ion, fragment ions	1–10	Measures intact molecule, small sample size, short analysis time, derivatization not required	Currently no on-line separation for ESI-Orbitrap, need for internationally recognized standards, cannot access all positions without chemical preparation	[13,14]; this study

^{13}C -enriched compared to the other carbons when organisms were grown autotrophically, and the opposite trend held for amino acids grown heterotrophically (shown for alanine only in Fig. 1). In contrast to the ^{13}C -enrichment at the C-1 position noted for autotrophically synthesized alanine, alanine produced abiotically via Strecker synthesis is ^{13}C -depleted at the C-1 position [24] compared to its source carbon pool (cyanide in this case), suggesting that abiotic and biotic synthesis pathways impart distinct intramolecular signals that can be traced back to their source (Fig. 1). The ability to detect these intramolecular differences can provide valuable information about a molecule's synthesis relevant to planetary science, biomedical research, archaeology, and numerous other fields looking to obtain diagnostic signatures of specific processes.

Alanine was specifically selected as a test case for PSIA by ESI-Orbitrap-MS in this study for several reasons. First, it is easily soluble in water and methanol, both common solvents used for direct infusion of samples for ESI-Orbitrap-MS. Second, it ionizes well by electrospray ionization, producing a robust molecular ion, and collisional fragmentation yields a fragment that has lost the C-1 position. Third, alanine contains only three carbons, and its collisional fragmentation yields a relatively simple ion fragment spectrum. Fourth, it is relatively

straightforward to obtain standards with isotope enrichments at individual carbon positions, which can be used to confirm the atom position represented in each fragment ion.

Here, we use ESI-Orbitrap-MS to obtain the molecular average and position-specific carbon isotope composition of alanine rapidly, accurately, and precisely. The use of ^{13}C -labels allows for confirmation of hypothesized fragmentation patterns (i.e. [27], and lack of recombination. The precision we achieved demonstrates the ability to detect isotopic differences on an environmentally relevant scale (on the order of a few ‰). ESI-Orbitrap-MS measurements were validated by comparison to established isotope ratio mass spectrometry techniques: elemental analyzer isotope ratio mass spectrometry (EA-IRMS), gas chromatography isotope ratio mass spectrometry (GC-C-IRMS), and specialized gas chromatography pyrolysis gas chromatography IRMS (GC-Py-GC-C-IRMS) instrumentation at Tokyo Tech.

2. Methods

2.1. Preparation of ^{13}C -enriched alanine standards

Twelve alanine standards were prepared with different amounts of

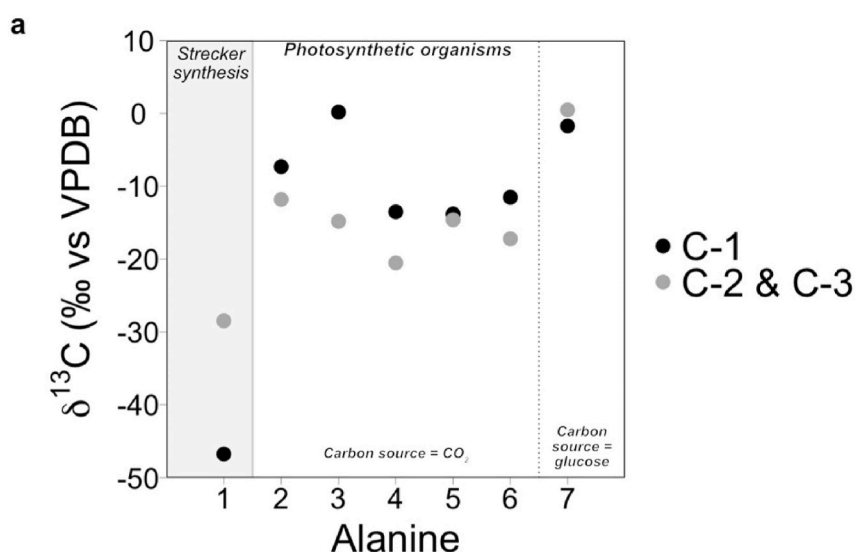
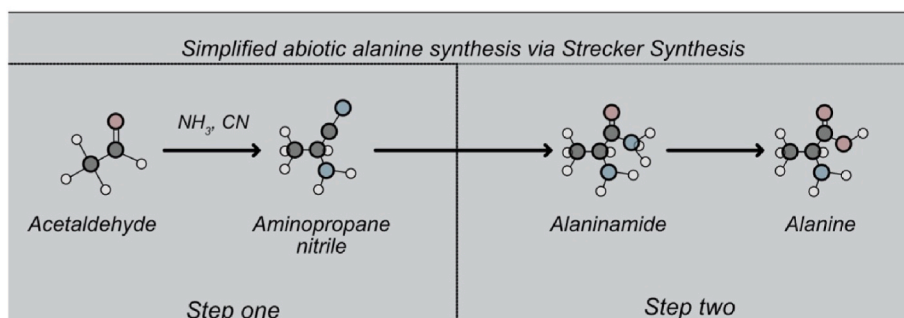
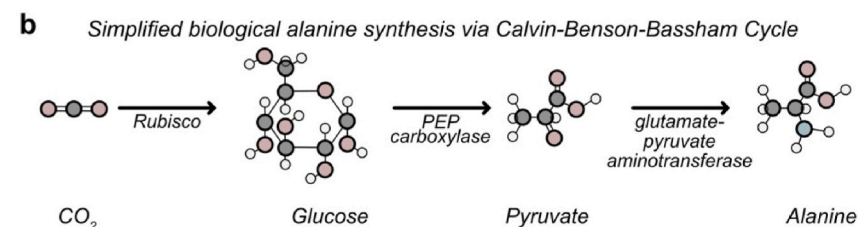


Fig. 1. Panel a shows a comparison of abiotic alanine from Strecker synthesis (shaded panel, data from Ref. [24]) and biological alanine from five photosynthetic organisms grown on CO_2 , and one grown on glucose (unshaded panel, data from Ref. [2]). Alanine produced by Strecker synthesis has a more ^{13}C -depleted signal overall and specifically leads to a C-1 position that is ^{13}C -depleted relative to the other carbon positions. Biologically derived alanine from photosynthetic organisms is ^{13}C -enriched at the C-1 position relative to the combined C-2 and C-3 positions. The species in the unshaded part of the figure use the Calvin-Benson-Bassham cycle for CO_2 fixation and are as follows: 2: *Chlorella pyrenoidosa* grown on CO_2 ; 3: *Anacystis nidulans* grown on CO_2 ; 4: *Scenedesmus quadricauda* grown on CO_2 ; 5: *Euglena gracilis* grown on CO_2 ; 6: *Gracilaria* sp. Grown on CO_2 ; 7: *Chlorella pyrenoidosa* grown on glucose. Panel b demonstrates the simplified pathways of biological and abiotic formation of alanine.



^{13}C -enrichment at each of the individual carbon positions (Fig. 2). Four different L-alanine standards were purchased to make the ^{13}C -enriched standards. The natural abundance L-Alanine was purchased from Sigma-Aldrich (Lot # MKCD3291). The three ^{13}C -labeled (99%) L-alanine standards purchased from Cambridge Isotope Laboratories Inc. had the following lot numbers: C-1: Lot # PR-20861, C-2: Lot # PR-19480, C-3: Lot # PR-26383. Enriched alanine standards were prepared by mixing small amounts of alanine containing a $>99\%$ ^{13}C -label at a specific carbon position (C-1, C-2, or C-3) with alanine at natural carbon isotope abundance (named “Natural Abundance Standard” in Table 2) in 50 mL conical Falcon centrifuge tubes (dilution factor >1000). Then, 20 mL of MilliQ water was added. Four different dilutions were prepared from this stock solution (letters a to d in Table 2). The standards were then dried using a SpeedVac vacuum concentrator at 40°C under vacuum (50 mPa). Molecular average carbon isotope values span a $\sim 14\%$ range (Table 2) when measured by EA-IRMS. The position-specific variation covers an $\sim 35\text{--}45\%$ range at each individual position.

2.2. EA-IRMS

The molecular average carbon isotope composition ($\delta^{13}\text{C}_{\text{MA}}$) of the alanine standards was characterized by EA-IRMS at Caltech and Tokyo Tech (Fig. 2b).

2.2.1. Caltech

At Caltech the $\delta^{13}\text{C}_{\text{MA}}$ values of the alanine standards were measured with an isotope ratio mass spectrometer (DELTA V, Thermo Fisher Scientific) connected to a combustion elemental analyzer (EA Isolink, Thermo Fisher Scientific) via a continuous flow interface (ConFlo IV, Thermo Fisher Scientific). In this system, standards wrapped in tin capsules were combusted at 1020°C with tungsten oxide as the oxidizer. Water was removed as the effluent stream passed through a water trap installed immediately after the reduction column. The N_2 and CO_2 peaks were separated on a gas chromatographic column (3 mm \times 90 cm NCS column) operated at 50°C . Two calibrated standards were used: natural abundance alanine ($\delta^{13}\text{C}_{\text{VPDB}} = -12.01\%$) and USGS 66 glycine ($\delta^{13}\text{C}_{\text{VPDB}} = -0.67\%$). Standards were analyzed in triplicate and $\delta^{13}\text{C}_{\text{MA}}$ values (Table 2 and Fig. 2b) are the average of the three analyses.

2.2.2. Tokyo Tech

At Tokyo Tech, the $\delta^{13}\text{C}_{\text{MA}}$ values of the alanine standards were measured with an isotope ratio mass spectrometer (DELTA XL, Thermo Fisher Scientific) connected to an elemental analyzer (EA 1108, CE Instruments) with a continuous flow interface (ConFlo II, Thermo Fisher

Scientific). In this system, samples wrapped in tin capsules were combusted at 1020°C . The combustion products were then transferred by a carrier gas (He) to the reduction column with reduced copper at 780°C for the reduction of nitrogen oxides to N_2 . Water was removed as the effluent stream passed through a water trap column installed immediately after the reduction column. The N_2 and CO_2 peaks were separated on a gas chromatographic column (6 mm \times 3 m, CE Instruments) operated at 50°C . Each standard was measured three times and data were calibrated by comparison with IAEA 600 (caffeine, $\delta^{13}\text{C}_{\text{VPDB}} = -27.77\%$) and a lab standard (sucrose, $\delta^{13}\text{C}_{\text{VPDB}} = -13.36\%$).

2.3. Isotope analysis by ESI-Orbitrap-MS

The twelve alanine standards (Table 2) were analyzed under two different instrument settings in triplicate on a Q Exactive HF OrbitrapTM mass spectrometer with an electrospray ionization source (ESI-Orbitrap-MS) to obtain molecular average and position-specific isotope values. The natural abundance (NA) alanine was used as a bracketing standard. 0.45 mg of alanine was dissolved in milliQ water and prepared in a water:methanol solution (3:7 v/v) at a concentration of $50\ \mu\text{M}$ with 0.1% (by volume) formic acid added to help ionization. Standard solutions were introduced into the ESI-Orbitrap-MS using PEEK tubing connected to a syringe pump (direct infusion). Two separate sets of analyses were conducted to characterize the sum of all carbons in the molecule (molecular average, MA) and to constrain the C-1 position (M+1 analysis, position-specific isotope analysis, PSIA, section 2.3.2). Daily instrument conditions were monitored using an in-house acetate standard to assess electrospray ionization efficiency and stability.

2.3.1. Molecular average

The MA values were analyzed in three different ways: 1) for all 12 standards, using a high-flow needle with $5\ \mu\text{L}/\text{min}$ flow rate; 2) for several standards using a low-flow needle with $3\ \mu\text{L}/\text{min}$ flow rate; 3) for one standard only, using a dual syringe pump set up (as described in Ref. [23] with the low-flow needle at $3\ \mu\text{L}/\text{min}$ flow rate. We here present results for all standards obtained via method (1) (Table 2); we compare the alternative strategies in the SI (Fig. S1).

For method (1), A direct infusion of a $50\ \mu\text{M}$ solution of alanine in water:methanol:formic acid was introduced at a flow rate of $5\ \mu\text{L}/\text{min}$. The analysis bracket was performed as follows: the NA alanine standard was analyzed three times, then the ^{13}C -enriched standard three times, then the NA alanine standard three times. Data for a single analysis was acquired for 15 min, requiring $75\ \mu\text{L}$ ($3.75\ \text{nmol}$ of analyte). When switching between ^{13}C -enriched standard and NA alanine bracketing

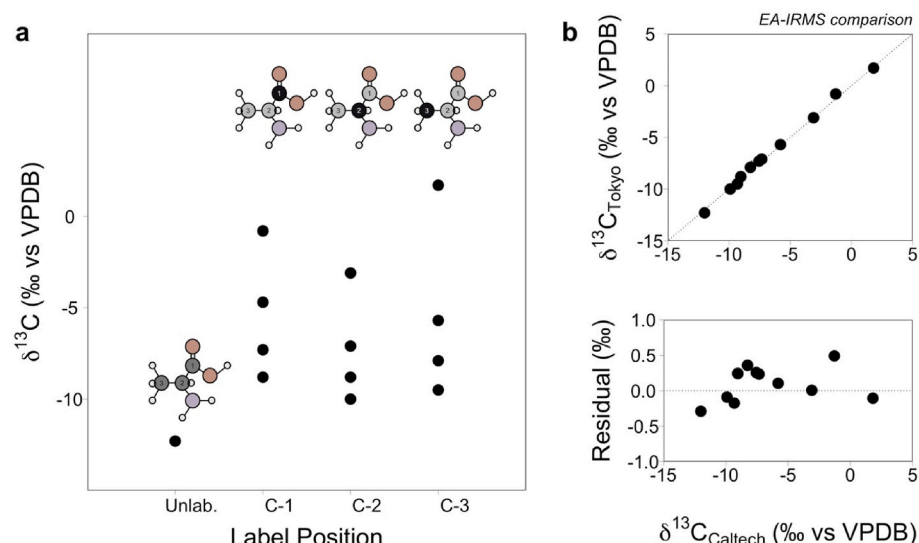


Fig. 2. Carbon isotopic compositions of alanine standards. Panel a: range of molecular average $\delta^{13}\text{C}$ values of each set of ^{13}C -enriched alanine standards. Panel b shows the comparison of the molecular average values measured by EA-IRMS at Caltech (x-axis) and Tokyo Tech (y-axis). All points fall on the 1:1 line within error and the offset between Caltech and Tokyo Tech values against the $\delta^{13}\text{C}$ values measured at Caltech is shown in the bottom portion of panel b. There does not appear to be a systematic offset based on $\delta^{13}\text{C}$ value.

Table 2

Molecular average (MA) and position-specific (PSIA) $\delta^{13}\text{C}$ values of the natural abundance standard and ^{13}C -enriched alanine standards measured by EA-IRMS, ESI-Orbitrap-MS, GC-C-IRMS, and GC-Py-GC-C-IRMS. The shaded row represents the alanine standard without any enrichment that was used as a bracketing standard for ESI-Orbitrap-MS analyses. The letters a to d correspond to the level of ^{13}C -enrichment for the standards with standard-a being the most ^{13}C -enriched and d being the least. Values represent averages of all measurements for a given standard. The errors for the ESI-Orbitrap-MS analyses are the standard error of the delta values, also referred to as experimental reproducibility. The errors for the GC analyses are the standard deviations of replicates.

Name	Molecular Average Measurements						Position-Specific Measurements									
	Caltech EA-IRMS		Tokyo Tech EA-IRMS		ESI-Orbitrap-MS		GC-IRMS		GC-Py-GC-IRMS		GC-Py-GC-IRMS		ESI-Orbitrap-MS			
	$\delta^{13}\text{C}_{\text{MA}}$ (‰ vs VPDB)	S. E.	$\delta^{13}\text{C}_{\text{MA}}$ (‰ vs VPDB)	S. E.	$\delta^{13}\text{C}_{\text{MA}}$ (‰ vs VPDB)	S. E.	$\delta^{13}\text{C}_{\text{C-1}}$ (‰ vs unlab)	S. E.	$\delta^{13}\text{C}_{\text{C-2}}$ (‰ vs unlab)	S. E.	$\delta^{13}\text{C}_{\text{C-3}}$ (‰ vs unlab)	S. E.	$\delta^{13}\text{C}_{\text{C-1}}$ (‰ vs unlab)	S. E.	$\delta^{13}\text{C}_{\text{C-2 \& C-3}}$ (‰ vs unlab)	S. E.
Natural abundance (NA) Alanine Standard	−12.0	0.1	−12.3	0.1	n.m.	n.m.	−11.9	0.5	−12.9	0.2	−7.0	0.1	n.m.	n.m.	n.m.	n.m.
C-1a	−1.3	0.4	−0.8	0.1	−1.4	0.4	34.3	0.2	n.m.	n.m.	n.m.	n.m.	32.0	0.1	−0.8	0.0
C-1b	−6.3	0.3	−4.7	0.1	−4.5	0.2	22.6	0.2	n.m.	n.m.	n.m.	n.m.	19.5	0.1	0.6	0.0
C-1c	−7.6	0.6	−7.3	0.1	−6.3	0.6	15.4	0.3	n.m.	n.m.	n.m.	n.m.	15.9	0.1	−0.3	0.1
C-1d	−9.0	0.2	−8.8	0.1	−10.1	0.4	10.3	0.5	n.m.	n.m.	n.m.	n.m.	−1.2	0.6	2.4	0.3
C-2a	−3.1	0.3	−3.1	0.4	−3.7	0.2	0.0	0.4	30.2	0.1	−0.9	0.6	0.1	0.6	11.6	0.3
C-2b	−7.3	0.4	−7.1	0.1	−7.0	0.7	0.1	0.5	15.3	0.2	−0.6	0.4	−1.3	0.5	7.2	0.2
C-2c	−9.0	0.1	−8.8	0.1	−10.8	0.4	0.3	0.7	10.1	0.1	−0.7	0.3	−3.2	0.5	2.3	0.2
C-2d	−9.9	0.2	−10.0	0.1	−10.0	0.4	0.1	0.3	6.5	0.1	−1.0	0.2	1.1	1.4	1.4	0.7
C-3a	1.8	0.3	1.7	0.3	0.5	0.7	−0.2	0.4	0.5	0.2	45.4	0.5	−1.8	0.3	18.9	0.2
C-3b	−5.8	0.3	−5.7	0.1	−4.2	0.9	0.0	0.2	−0.2	0.1	20.4	0.4	2.1	0.5	9.7	0.2
C-3c	−8.3	0.2	−7.9	0.1	−6.9	0.4	−0.3	0.1	0.1	0.4	13.5	0.5	1.0	1.2	6.1	0.6
C-3d	−9.3	0.1	−9.5	0.2	−8.7	0.2	−0.3	0.3	−0.4	0.1	8.0	0.2	0.8	0.3	3.6	0.1

standard, the syringe was rinsed with 1.5 mL methanol and the PEEK tubing (connecting the syringe and source) was rinsed with 500 μL methanol. Separate syringes and tubing were used for each individual standard to ensure no carry-over of ^{13}C -enrichment between analyses. Rinsing with pure methanol between acquisitions resulted in blanks <5% of the analyte abundance, therefore no blank corrections were performed. Instrument parameters for MA analyses were as follows: a full scan of 85.5–95.5 m/z in positive polarity was performed with the unsubstituted (^{12}C) and single ^{13}C -substituted (^{13}C) ions falling in the center of the scan. The (nominal) resolution was set to 120,000 and Automatic Gain Control (AGC) Target was at 200,000. The resolution allowed for separation of the ^{13}C , ^{15}N , and ^2H peaks. Other source parameters were set as follows: Sheath gas flow = 3, Auxiliary gas flow = 0, Sweep gas flow = 0, Spray voltage = 4 kV, Capillary temperature = 320 $^{\circ}\text{C}$, S Lens RF = 60, Auxiliary gas heater = 40 $^{\circ}\text{C}$. These parameters can be modified as necessary to ensure the ions of interest are dominant and non-analyte peaks are minimized.

2.3.2. Position-specific isotope analysis

For PSIA, an aliquot of the same 50 μM solution of alanine in water: methanol:formic acid was infused into the instrument for 15 min at a flow rate of 20 $\mu\text{L}/\text{min}$. The same cleaning procedures used for MA analyses were employed. Bracketing took the form of alternating NA standard and ^{13}C -enriched standard acquisitions (i.e., NA alanine standard, ^{13}C -enriched standard, NA alanine standard, ^{13}C -enriched standard, etc.) so that ^{13}C -enriched standards were analyzed in triplicate. The isotopologues with a cardinal mass of 1 higher than the unsubstituted isotopologue (which we denote the “M+1” isotopologues”) were isolated by setting the quadrupole mass filter to select masses of 91 ± 0.5 m/z and sent into the higher-energy collision-induced dissociation (HCD) cell at a collision energy of 80 NCE. After being sent to the HCD cell, all produced fragment ions were injected into the Orbitrap for mass analysis (this combination of mass pre-selection followed by collision and Orbitrap analysis is hereafter referred to as “M+1 analysis”; Neubauer et al., 2018). A single dominant fragment ion was produced that

contained the C-2 and C-3 positions ($\text{C}_2\text{H}_6\text{N}$, Fig. 3, referred to as the “44 fragment” given the cardinal mass of the unsubstituted version is 44). Service mode was used to access the low mass range between 30 and 50 m/z . The 44 fragment analyses used the following parameters: the mass window of the quadrupole mass pre-selection was 91 ± 0.5 m/z , nominal mass resolution of 30,000, AGC target of 50,000. The AGC target determines how long ions must be accumulated in the C-Trap before transfer to the Orbitrap. A low AGC target was used for the M+1 analyses because the abundance of ions generated during fragmentation is much lower than for the molecular ion measurements and the lower

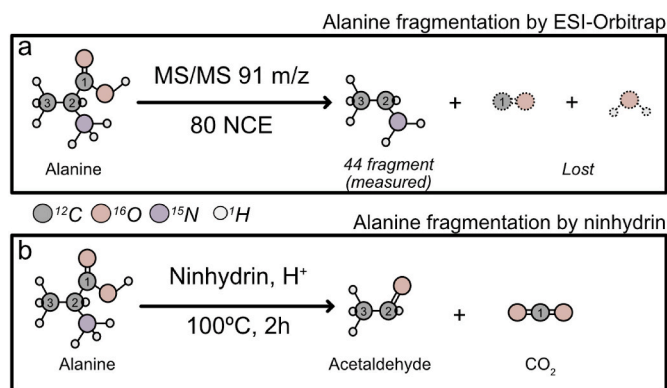


Fig. 3. To measure the intramolecular carbon isotope composition of alanine, it is necessary to break apart the molecule. Panel a: fragmentation of alanine by ESI-Orbitrap-MS. This instrument-based fragmentation uses the higher energy collisional dissociation (HCD) cell which causes loss of the C-1 position resulting in a fragment containing the C-2 and C-3 position. Panel b illustrates the Ninhydrin reaction adapted from Ref. [28] which is used to release the C-1 position as CO_2 prior to analysis by GC-IRMS. The Ninhydrin reaction generates CO_2 which contains the C-1 position of alanine and acetaldehyde which has the C-2 and C-3 carbons. Acetaldehyde is further separated on a GC-Py-GC-C-IRMS system which permits analysis of the C-2 and C-3 positions individually.

AGC target allowed for shorter accumulation time. Ion source parameters were set as follows: Sheath gas flow = 10, Auxiliary gas flow = 0, Sweep gas flow = 0, Spray voltage = 4 kV, Capillary temperature = 320 °C, S Lens RF = 60, Auxiliary gas heater = 40 °C. Additional tuning of C-Trap and Ion Optics radio frequencies (RF; accessed via service mode) allowed for an increased signal of the m/z 44 and 45 ions. The C-Trap RF II Supply RF amplitude was set at 520 Vpp and the Ion Optics RF 2/3 amplitude was set to 260 Vpp. Data for a single analysis was acquired for 15 min, requiring 300 μ L (15 nmol) of analyte.

2.4. Isotope analysis by isotope ratio mass spectrometry

PSIA of alanine was also performed using a three-step method: (i) the reaction of alanine with ninhydrin followed by (ii) the isotope analysis of evolved CO_2 representing the C-1 position (Fig. 3) and molecular average isotope analysis of generated acetaldehyde by GC-C-IRMS, and (iii) the intramolecular isotope analysis of acetaldehyde by GC-Py-GC-C-IRMS.

2.4.1. Ninhydrin reaction

For each standard, 4 mg of alanine was introduced into glass vials sealed with butyl rubber caps. Helium gas was flushed into the vials for 2 min to eliminate CO_2 from air. Two mL of Ninhydrin solution (3.5% of Ninhydrin and 1.1% H_3PO_4) was added using a syringe and the reaction was conducted at 100 °C for 2h. This reaction converts alanine into CO_2 (corresponding to the C-1 position of alanine, Fig. 3) and acetaldehyde (containing C-2 and C-3 of alanine, Fig. 3).

2.4.2. Molecular average carbon isotope analysis of CO_2 and acetaldehyde

The molecular average carbon isotope values of both CO_2 and acetaldehyde were determined using a gas chromatograph coupled with the isotope ratio mass spectrometer (DeltaPlusXP, Thermo Fisher Scientific) via a combustion furnace and an open split interface (GC Combustion III, Thermo Fisher Scientific). High-purity helium (>99.99%) was used as a carrier gas. CO_2 was injected into the GC equipped with a capillary column (Stabilwax, 30 m \times 0.32 mm i. d., 10 μ m film thickness; Varian, CA, USA) using a gas-tight syringe and the conditions were as follows: injector temperature 300 °C; split ratio 40:1; flow rate at 1.5 mL/min; oven temperature was maintained at 50 °C until CO_2 elution.

The procedure for extracting acetaldehyde in the gas phase from ninhydrin reaction products was performed using solid-phase microextraction (SPME), carried out for 5 min at ambient temperature using an 85 μ m SPME fiber coated with carboxen/polydimethylsiloxane (Carboxen/PDMS StableFlex; Supelco). SPME was then introduced in the same GC system as CO_2 and the separation conditions were as follows: injector temperature 300 °C; split ratio 10:1; flow rate at 1.5 mL/min; oven temperature was maintained at 60 °C for 6 min then raised to 250 °C (30 °C/min) and this temperature was maintained for 5 min. The SPME was kept in the injector during the analysis in order to optimize acetaldehyde desorption and avoid memory effects. After leaving the GC, the effluent entered a combustion furnace (operated at 960 °C) containing a ceramic tube packed with CuO, NiO, and Pt wires. The generated CO_2 was then analyzed in the IRMS. Isotopic standardization was made by CO_2 injections calibrated against the natural gas standard NGS-2 provided by the National Institute of Standards and Technology (NIST), Gaithersburg, MD, USA.

2.4.3. Position-specific isotope analysis of acetaldehyde

The online pyrolysis method used in this study, initially developed during the 1990s [5,29] and more recently adapted to the position-specific isotope analysis of propane [7] and butane isomers [30], is described in this section. To access the intramolecular isotopic composition of acetaldehyde, an online pyrolysis system and a second GC were coupled to the GC-C-IRMS described above. Acetaldehyde was extracted from the gas phase using the same method as the molecular average isotope analysis for 10 min at ambient temperature. Solid phase

microextraction (SPME) was then introduced into the injector (300 °C; split ratio 5:1) and acetaldehyde was isolated using a first GC column (Stabilwax, 30 m \times 0.32 mm i. d., 10 μ m film thickness; Varian, CA, USA) maintained at 60 °C for 10 min then raised to 250 °C (30 °C/min). Acetaldehyde was transferred to a high-temperature conversion furnace (deactivated fused silica capillary column 0.32 mm i. d. Inserted into a ceramic tube of 25 cm \times 0.5 mm i. d.) operating at 1000 °C. Fragments generated through pyrolysis were then separated in a second GC column (HP-PLOT-Q, 30 m \times 0.32 mm i. d., 10 μ m film thickness; Varian, CA, USA) as follows: 35 °C for 15 min, then raised to 150 °C (30 °C/min) and held for 5 min. Each fragment was finally converted into CO_2 in the combustion furnace and analyzed in the IRMS. Isotopic standardization was made by CO_2 injections calibrated against the natural gas standard NGS-2 provided by the National Institute of Standards and Technology (NIST), Gaithersburg, MD, USA.

2.5. Data processing

2.5.1. MA by ESI-Orbitrap-MS

Isotope ratios were computed as follows using Eqn. (1) [13]:

$$\text{counts} = \left(\frac{S}{N} \right) \left(\frac{C_N}{z} \right) \sqrt{\frac{\text{Res}_N}{\text{Res}}} \quad (1)$$

where S is ion intensity, N is peak noise, C_N is an empirical factor of 2.7 determined by Ref. [31]; z is the ion's charge, Res_N is the reference resolution, and Res is the resolution setting on the instrument used for the analyses. Then, isotope ratios for each scan (R_{scan}) were determined as the ratio of counts of the heavy ion to counts of the unsubstituted ion, e.g.:

$$R_{\text{scan}} = \frac{\text{counts}^{13}\text{C}_{\text{scan}}}{\text{counts}^{12}\text{C}_{\text{scan}}} \quad (2)$$

where the ^{12}C counts were derived using data for the unsubstituted peak ($^{12}\text{C}_3\text{H}_8\text{NO}_2$, 90.05550 m/z) and the ^{13}C counts correspond to the singly ^{13}C -substituted peak ($^{12}\text{C}_2^{13}\text{CH}_8\text{NO}_2$, 91.05886 m/z). We then calculated the average ratio across all scans of the acquisition ($R_{\text{acquisition}}$) and the standard error of this ratio across all scans σ_{AE} , which we call the 'acquisition error':

$$R_{\text{acquisition}} = \frac{\sum_{i=1}^N R_{\text{scan}}^{13\text{C}}}{N} \quad (3)$$

$$\sigma_{\text{AE}} = \frac{SD(R_{\text{scan}}^{13\text{C}})}{\sqrt{N}} \quad (4)$$

An alanine internal standard having a natural abundance of ^{13}C ("NA alanine Standard" in Table 2) was analyzed alongside the ^{13}C -enriched alanine standards. We first averaged the ratios across the 3 ^{13}C -enriched standards ($R_{\text{AVG,Sample}}$) and 6 NA alanine standard acquisitions ($R_{\text{AVG,Standard}}$). We then determined the experimental reproducibility (precision) of the ratios ($\sigma_{\text{ER,ratio}}$) and of the delta values ($\sigma_{\text{ER,delta}}$) by taking the standard error of all six standard ratios or deltas and the standard error of all three ^{13}C -enriched standard ratios or deltas and adding the errors for both ^{13}C -enriched standard and natural abundance standard acquisitions in quadrature:

$$\sigma_{\text{ER,ratio}} = \sqrt{\left(\frac{SD(R_{\text{AVG,SMP}})}{\sqrt{N}} \right)^2 + \left(\frac{SD(R_{\text{AVG,STD}})}{\sqrt{N}} \right)^2} \quad (5)$$

$$\sigma_{\text{ER,delta}} = \sqrt{\left(\frac{SD(\delta_{\text{AVG,SMP}})}{\sqrt{N}} \right)^2 + \left(\frac{SD(\delta_{\text{AVG,STD}})}{\sqrt{N}} \right)^2} \quad (6)$$

All delta values are anchored to VPDB, reported in ‰, and errors in Table 2 and Fig. 6 reflect the experimental reproducibility of the delta values (Eqn. (6)). Note that comparison of this Orbitrap-based MA measurement with independent EA-based measurements of molecular

average $\delta^{13}\text{C}$ implicitly assume that ^{13}C -enriched standard and natural abundance standard have similar probabilities of double and higher-order ^{13}C substitutions (i.e., we use the singly substituted species as proxies for overall $^{13}\text{C}/^{12}\text{C}$ abundance ratios).

Using the R value of 0.011099 for the natural abundance standard determined by EA-IRMS, we converted ESI-Orbitrap-MS R values for MA measurements onto the VPDB scale in Table 2:

$$\frac{R_{\text{AVG,Samp,Orbi}}}{R_{\text{AVG,Std,Orbi}}} * R_{\text{AVG,Std,EA}} \quad (7)$$

2.5.2. PSIA by ESI-Orbitrap-MS

Our PSIA measurement incorporates both observations of the 44 fragment (lacking the carboxyl moiety) and the MA measurement. This method includes the following: 1) a “M+1” analysis of the 44 fragment which determines the distribution of M+1 substitutions within the fragment ions, 2) a “M+1” analysis of the previously discussed MA dataset (that is, the same data, processed to compute the amounts of ^{13}C , ^{15}N , and ^2H relative to each other, and ignoring the unsubstituted ion), 3) The MA dataset as presented in 2.5.1, above. We use (1) and (2) to compute the distribution of carbon between different positions, then scale this distribution using the known amount of ^{13}C from (3) to determine the amount of ^{13}C at each carbon position. An overview of measurements and calculations are shown in Fig. 4, elaborated upon in Ref. [32]; and discussed further below. We chose to perform this M+1

analysis rather than fragmenting with the unsubstituted isotopologue because the M+1 strategy causes increase in the relative intensity of the singly substituted species (M+1) compared to the unsubstituted, allowing for more counts of the rare isotope and therefore a more rapid measurement [14].

For the M+1 analyses (1) and (2) we began by calculating counts of each ion beam for both the 44 fragment (M+1) and the full molecule (MA). Then, for each scan, we calculated M+1 relative abundances ρ , or the ratios of the intensities of a given M+1 ion relative to the intensities of all ions in the M+1 population. These can be thought of as capturing the distribution of heavy isotopes within the M+1 population. For example, for using the 44 fragment and the ^{13}C ion this is:

$$\rho_{44,\text{scan}}^{13\text{C}} = \frac{\text{counts}^{13\text{C}}_{\text{scan}}}{\text{counts}_{\text{Unsub}_{\text{scan}}} + \text{counts}^{13\text{C}}_{\text{scan}} + \text{counts}^{15\text{N}}_{\text{scan}} + \text{counts}^2\text{H}_{\text{scan}}} \quad (8)$$

Or for the full molecule:

$$\rho_{\text{full},\text{scan}}^{13\text{C}} = \frac{\text{counts}^{13\text{C}}_{\text{scan}}}{\text{counts}^{13\text{C}}_{\text{scan}} + \text{counts}^{15\text{N}}_{\text{scan}} + \text{counts}^2\text{H}_{\text{scan}}} \quad (9)$$

Note that for the 44 fragment, the ^{12}C (unsubstituted) peak is included in the denominator, while in the full molecule the unsubstituted peak is not included. For the M+1 analyses, the heavy substitutions (^{13}C , ^{17}O , ^2H) may be lost upon fragmentation, generating unsubstituted peaks which are included in the M+1 calculations (purple box, Fig. 4). In the M+1 analysis of the 44 fragment, this occurs when the heavy substitutions are present in the CO or H₂O lost upon fragmentation (see Fig. 3a); in contrast, in the M+1 analysis of the full molecule (green box, Fig. 4), this does not occur, so no unsubstituted peaks are observed. We then calculate averages and standard errors of the M+1 relative abundances across all scans as was done for the full molecule (Eqns. (2)–(7)). We standardize these values using a forward model and standard brackets following the methods in Ref. [32]; and use these ρ values to calculate M+1 relative abundances at individual positions using matrix inversion:

$$\begin{pmatrix} 1 & 1 & 1 & 1 & 1 & 1 \\ 0 & 0 & 0 & 0 & 1 & 1 \\ 0 & 0 & 1 & 0 & 0 & 0 \\ 1 & 1 & 0 & 0 & 0 & 0 \\ 0 & 0 & 0 & 0 & 1 & 0 \\ 0 & 0 & 1 & 0 & 0 & 0 \\ 0 & 1 & 0 & 0 & 0 & 0 \\ 1 & 0 & 0 & 1 & 0 & 1 \end{pmatrix} \begin{pmatrix} \rho_{\text{carboxyl}}^{13\text{C}} \\ \rho_{\text{full}}^{13\text{C}} \\ \rho_{\text{full}}^{15\text{N}} \\ \rho_{\text{full}}^{13\text{C}} \\ \rho_{\text{amine}}^{15\text{N}} \\ \rho_{\text{carboxyl}}^{17\text{O}} \\ \rho_{\text{retained}}^{2\text{H}} \\ \rho_{\text{lost}}^{2\text{H}} \end{pmatrix} = \begin{pmatrix} 1 \\ \rho_{\text{full}}^{2\text{H}} \\ \rho_{\text{full}}^{15\text{N}} \\ \rho_{\text{full}}^{13\text{C}} \\ \rho_{44}^{2\text{H}} \\ \rho_{44}^{15\text{N}} \\ \rho_{44}^{13\text{C}} \\ \rho_{44}^{\text{Unsub}} \end{pmatrix}$$

The left matrix shows where isotope substitutions occur, the center column gives the isotopologues of interest, and the right column contains observed M+1 relative abundances of specific isotopologues. The data processing algorithm uses the *numpy.linalg.lstsq* python function to find a least-squares solution to the matrix equation and determine M+1 relative abundances [32].

The ρ values calculated via matrix inversion capture the distribution of M+1 substitutions between different sites but say nothing about the absolute amount of any substitution; we next add this information by scaling with a constant. Our mathematics use several “U” values, which are defined as the ratio between the concentrations of some set of isotopologues and the unsubstituted isotopologue.

We first define a U^{M+1} value [32], giving the ratio of all M+1 substituted isotopologues to unsubstituted isotopologues

$$U^{M+1} = \frac{^{15}\text{N} + ^{13}\text{C} + ^{17}\text{O} + ^2\text{H}}{\text{Unsub}} \quad (10)$$

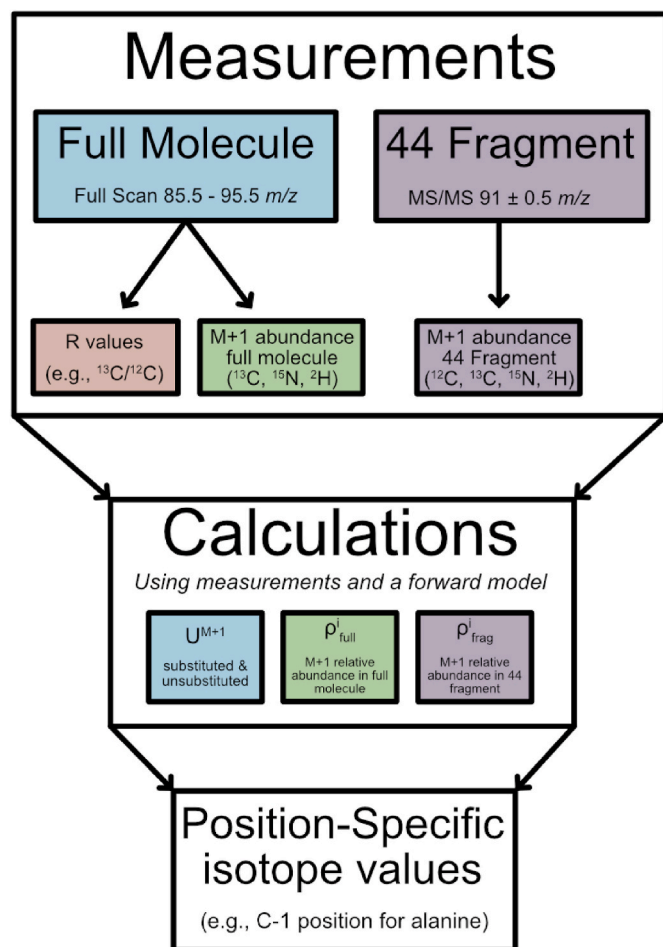


Fig. 4. Flow chart for MA and PSIA analysis by ESI-Orbitrap-MS. The full molecule and fragment(s) are measured, and that data is used to calculate U and ρ values which are converted into position-specific isotope values. Information about the measurement to calculation pipeline is outlined in section 2.5.2 and described in further detail in Ref. [32].

We calculate the U^{M+1} value using the MA measurement, via:

$$U^{M+1} \approx \frac{3 * R^{13C}}{\rho_{full}^{13C}} \quad (11)$$

Where the approximation holds as

$$U^{M+1} = \frac{U^{13C}}{\rho_{full}^{13C}} = \frac{\frac{[13C]}{[Unsub]}}{\frac{[13C]}{[M+1 \text{ Isotopologues}]}} = \frac{[M+1 \text{ Isotopologues}]}{[Unsub]} \quad (12)$$

and $R^{13C} \approx \frac{U^{13C}}{3}$ (the factor of 3 comes from the 3 carbon atoms in alanine). The numerator of the U^{M+1} and denominator of the ρ values correspond to the same isotopologues, so we can determine position-specific ratios by scaling the ρ values from our matrix inversion with the U^{M+1} value. For example, for the C-1 position:

$$\begin{aligned} \rho_{C-1}^{13C} * U^{M+1} &= \frac{[13C]_{C1}}{[M+1 \text{ Isotop.}]} * \frac{[M+1 \text{ Isotop.}]}{[Unsub]} = \frac{[13C]_{C1}}{[Unsub]} = U^{13C,C-1} \\ &\approx n * R^{13C,C1} \end{aligned} \quad (13)$$

Where n is the number of atoms at the C-1 position.

These values may be reported as delta values in the relevant reference frame; for example, for C-1: $1000 * \left(\frac{R^{13C,C1}}{R^{13C}_{std}} - 1 \right)$. The M+1 data processing algorithm provides four different outputs: two using the natural abundance alanine as the reference standard and two linking the PSIA measurements to the VPDB scale. For both reference frames, the ESI-Orbitrap-MS or the EA-IRMS molecular average values can be used for calculating position-specific values. The difference between the ESI-Orbitrap-MS values and the corresponding IRMS measurements for all four calculations are shown in Fig. S2. For the discussion and figures in the main manuscript, the position-specific δ^{13C} values are calculated using ESI-Orbitrap-MS molecular average values relative to the natural abundance standard. Our implementation of this method is publicly available at <https://doi.org/10.22002/xz4cp-hyd02>.

2.5.3. Tokyo Tech pyrolysis GC analyses

The pyrolysis of acetaldehyde generates CH_4 (23%), CO (60%), C_2H_4 (11%) and C_2H_6 (7%). These mole basis percentages were calculated ($n = 26$) using m/z 44 peak areas corrected according to the carbon number of the considered compounds (e.g., area of ethane peak = area 44/2). Data provided by the analysis of the ^{13}C -enriched standards accompanied with predictions detailed in the following equations will help to elucidate the fragmentation mechanism and calibrate the isotope measurements. Equations (14)–(28) were designed to correct for any isotope effect associated with both the pyrolysis and the ninhydrin reaction. In the following equations, δ^{13C}_{C-3} , δ^{13C}_{C-2} , and δ^{13C}_{C-1} are the δ^{13C} values of methyl (C-3), central amine (C-2) and carboxyl (C-1) positions of alanine, respectively.

$$\delta^{13C}_{Ala} = \frac{\delta^{13C}_{C-1} + \delta^{13C}_{C-2} + \delta^{13C}_{C-3}}{3} \quad (14)$$

$$\delta^{13C}_{CO2} = \delta^{13C}_{C-1} \quad (15)$$

$$\delta^{13C}_{CO} = \delta^{13C}_{C-2} \quad (16)$$

$$\delta^{13C}_{CH4} = \delta^{13C}_{C-3} \quad (17)$$

$$\delta^{13C}_{acetaldehyde} = \delta^{13C}_{C2H4} = \frac{\delta^{13C}_{C-3} + \delta^{13C}_{C-2}}{2} \quad (18)$$

$$\delta^{13C}_{Ala} = \frac{2 * \delta^{13C}_{acetaldehyde} + \delta^{13C}_{CO2}}{3} \quad (19)$$

Previous studies of propane [7] and butane isomers [30] suggest recombination of methyl radicals is expected to lead to the formation of ethane (C_2H_6).

$$\delta^{13C}_{C2H6} = \delta^{13C}_{CH4} = \delta^{13C}_{C-3} \quad (20)$$

$$\delta^{13C}_{CO} = 2 * \delta^{13C}_{acetaldehyde} - \delta^{13C}_{CH4} \quad (21)$$

$$\delta^{13C}_{CH4} = 2 * \delta^{13C}_{acetaldehyde} - \delta^{13C}_{CO} \quad (22)$$

Fig. 5 presents some correlations between δ^{13C} values of fragments, δ^{13C}_{MA} values, and the acetaldehyde produced during the ninhydrin reaction. The correlations for CO_2 and the CO fragment were obtained using the standards with different ^{13}C -enrichments at the C-1 and C-2 positions respectively. The correlations for CH_4 and C_2H_6 fragments were obtained using the standards ^{13}C -enriched on the terminal C-3 position. These ^{13}C -enriched standards allow an understanding of which alanine positions are retained in fragments generated from the ninhydrin reaction and subsequent pyrolysis. As only one of three carbon positions is enriched in each standard, this kind of plot should have a slope equal to 3 when comparing δ^{13C}_{MA} values of alanine and δ^{13C} values of a fragment, or a slope of 2 when δ^{13C}_{MA} values of acetaldehyde are compared with δ^{13C} values of a fragment containing the ^{13}C -enriched position.

We conclude that the CO_2 (generated from reaction of alanine with ninhydrin) directly comes from the $COOH$ group (C-1 position) of alanine because the slope is very close to 3 (2.94 in Fig. 5a). Also, this result demonstrates the absence of an isotope effect associated with the ninhydrin reaction and no significant air contamination during the reaction, and the δ^{13C}_{C-1} value can be expressed as described in equation (15).

The linear relationship between CO data and δ^{13C}_{MA} values of alanine has a slope of 3.26 which is slightly higher than the theoretical slope (Fig. 5b). However, correlation of δ^{13C} values of CO and acetaldehyde (theoretical slope = 2, Fig. 5d) results in a slope of 1.91 suggesting that 96% of the CO directly originates from the central carbon position of alanine, so δ^{13C}_{C-2} values can be expressed as follows:

$$\delta^{13C}_{C-2} = \delta^{13C}_{CHO} = \delta^{13C}_{CO} \quad (23)$$

where δ^{13C}_{CHO} is the δ^{13C} of the aldehyde of acetaldehyde. Offsets from theoretical predictions are observed in plots comparing the δ^{13C} of CH_4 with both alanine and acetaldehyde. The correlation between δ^{13C}_{CH4} and δ^{13C}_{MA} has a slope of 2.77 instead of 3 (see Fig. 5c) and a slope of 1.69 is calculated for the relationship between δ^{13C}_{CH4} and $\delta^{13C}_{acetaldehyde}$ (Fig. 5f) when a slope of 2 is expected. These results suggest the presence of recombination during the pyrolysis of acetaldehyde, so corrections are required to represent true values. The slope of 1.69 [$\delta^{13C}_{CH4} = f(\delta^{13C}_{acetaldehyde})$, Fig. 5f] demonstrates that 85% (1.69/2) of CH_4 directly originates from the terminal CH_3 position of acetaldehyde during the pyrolysis and 15% comes from another source. Two carbon sources can generate fragments during the pyrolysis of acetaldehyde: the CH_3 (C-3) and the CHO (C-2) of acetaldehyde. In this context, 85% of CH_4 should be generated from CH_3 and 15% from CHO , so the following equation can be written:

$$\delta^{13C}_{CH4} = 0.85 * \delta^{13C}_{C-3} + 0.15 * \delta^{13C}_{CHO} \quad (24)$$

According to equations (23) and (24), δ^{13C}_{CH4} can be expressed as follows:

$$\delta^{13C}_{CH4} = 0.85 * \delta^{13C}_{C-3} + 0.15 * \delta^{13C}_{CO} \quad (25)$$

Finally, δ^{13C}_{CH3} of alanine (and acetaldehyde) can be calculated using the following equation:

$$\delta^{13C}_{C-3} = \frac{\delta^{13C}_{CH4} - 0.15 * \delta^{13C}_{CO}}{0.85} \quad (26)$$

In addition, the correlation $\delta^{13C}_{C2H6} = f(\delta^{13C}_{CH4})$ has a slope of 1.13 (Fig. 5e) which is close to the theoretical slope of 1 and proves that ethane is formed by recombination of methyl radicals during the pyrolysis as previously observed [7,30].

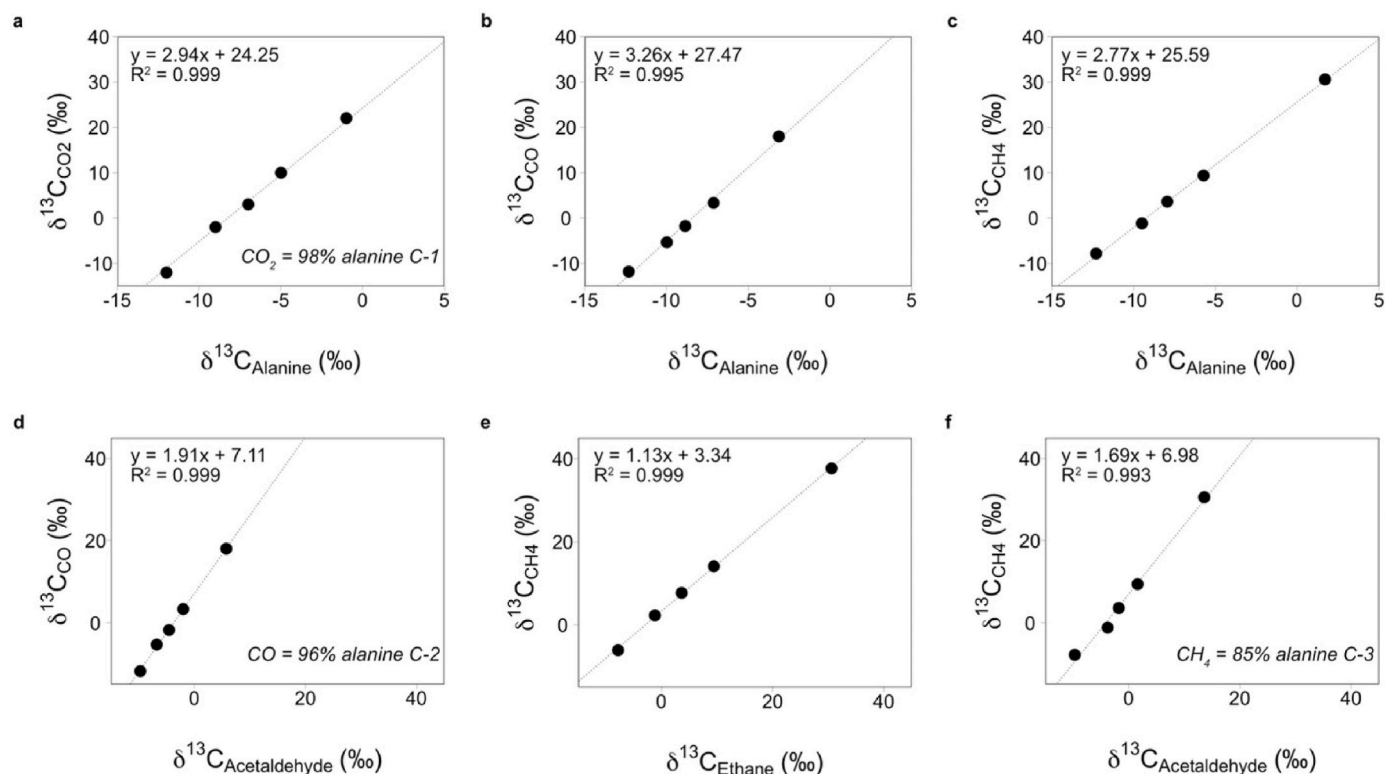


Fig. 5. Relationships between $\delta^{13}\text{C}$ values of the whole alanine molecule, acetaldehyde, and ethane with fragments produced by ninhydrin reaction (CO_2) and pyrolysis at 1000°C (CO , CH_4 and C_2H_6). These correlations are used to determine which positions from the original alanine molecule end up in which products.

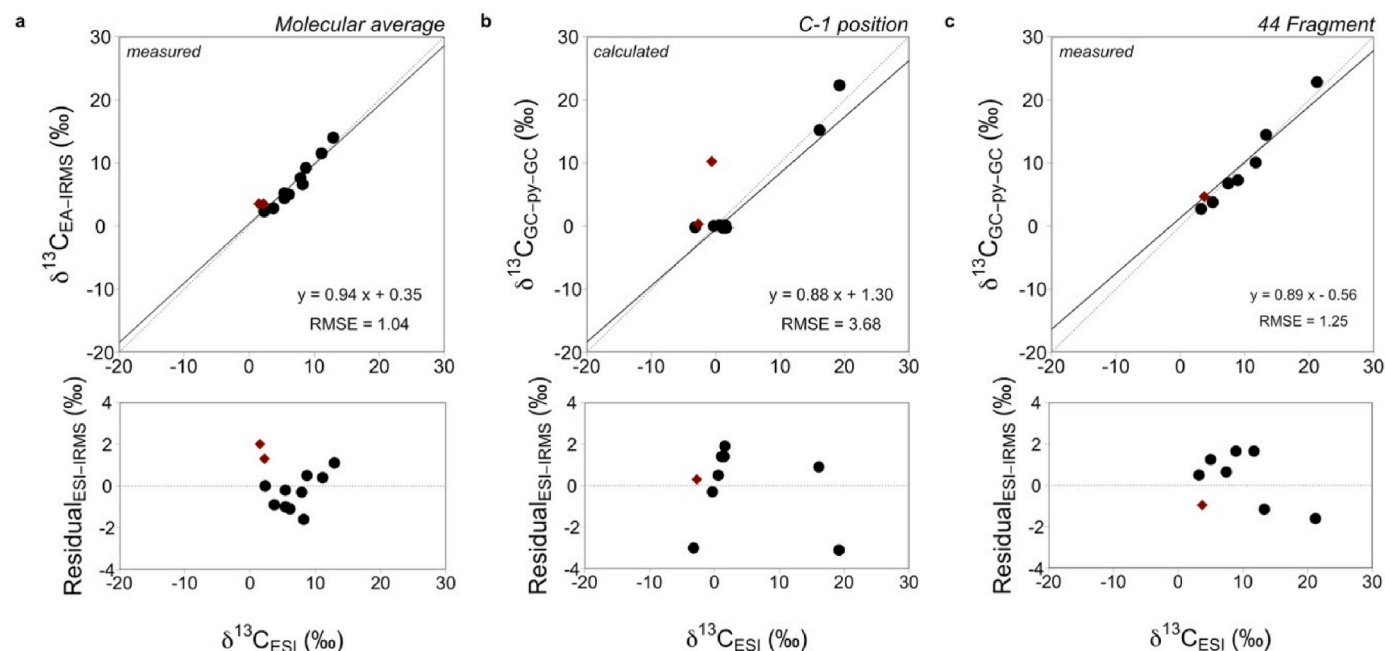


Fig. 6. Comparison of ESI-Orbitrap-MS data with EA-IRMS (a), GC-IRMS (b), and GC-Py-GC-C-IRMS (c). ESI-Orbitrap-MS values agree within error with values from established IRMS techniques for molecular average, C-1 position, and averaged C-2 and C-3 positions. The red diamonds indicate the two standards with the same molecular average value but different position-specific values. The solid line in each plot is the best fit linear regression and the dotted line is the 1:1 line.

To ensure data accuracy, both the $\delta^{13}\text{C}_{\text{MA}}$ of acetaldehyde and the $\delta^{13}\text{C}$ of pyrolytic fragments were directly compared to measurements of an acetaldehyde internal standard measured by GC-C-IRMS analysis (for $\delta^{13}\text{C}_{\text{MA}}$) and off-line pyrolysis followed by off-line combustion and IRMS analysis (for $\delta^{13}\text{C}_{\text{CO}}$ and $\delta^{13}\text{C}_{\text{CH}_4}$). The comparison of these data with

those obtained by GC-Py-GC-C-IRMS at 1000°C allows for the following correction factors to be determined: -1.1‰ for the CO and -0.1‰ for the CH_4 generated during the pyrolysis of acetaldehyde. Using the correction for the scrambling during pyrolysis and the correction factors calculated above, $\delta^{13}\text{C}_{\text{C-1}}$ is calculated using equation (15) ($\delta^{13}\text{C}_{\text{C-1}} =$

$\delta^{13}\text{C}_{\text{CO}_2}$). The two other positions, $\delta^{13}\text{C}_{\text{C-3}}$ and $\delta^{13}\text{C}_{\text{C-2}}$, of alanine are calculated as follows:

$$\delta^{13}\text{C}_{\text{C-2}} = \delta^{13}\text{C}_{\text{CO}} - 1.1 \quad (27)$$

$$\delta^{13}\text{C}_{\text{C-3}} = (\delta^{13}\text{C}_{\text{CH}_4} - 0.15 \times \delta^{13}\text{C}_{\text{CO}})/0.85 - 0.1 \quad (28)$$

Corrected data of the natural abundance and the ^{13}C -enriched alanine standards measured by GC-C-IRMS ($\delta^{13}\text{C}_{\text{MA}}$) and GC-Py-GC-C-IRMS ($\delta^{13}\text{C}$ of the three individual carbon positions of alanine) are summarized in Table 2.

3. Results and discussion

Molecular average and position-specific carbon isotope values were measured for twelve ^{13}C -enriched alanine standards using ESI-Orbitrap-MS, EA-IRMS, GC-C-IRMS, and GC-Py-GC-C-IRMS instrumentation (Table 2, Figs. 2 and 6). The molecular average values for all standards were determined by EA-IRMS at Caltech and Tokyo Tech. Values from both sets of analyses agree within analytical uncertainty (Fig. 2b). Root-mean-square error (RMSE) analysis (i.e., accuracy) between the two EA-IRMS datasets is 0.52‰. Molecular average values were also measured by ESI-Orbitrap-MS (Fig. 6a). The shot noise error for MA measurements is $\leq 0.22\text{‰}$ and experimental reproducibility of delta values (SE in Table 2) was between 0.2 and 0.9‰, close to shot noise limit. RMSE for ESI-Orbitrap-MS MA values was 1.0‰ with $<1\text{‰}$ precision.

Position-specific isotope values were measured by a three-step GC-IRMS method and used as validation of the two-step ESI-Orbitrap-MS measurements. Linear regressions for comparison of IRMS and ESI-Orbitrap-MS analyses for MA, C-1, and the 44 fragment resulted in equations shown in Fig. 6. The deviation of ESI-Orbitrap-MS values from IRMS values does not appear to be systematic (Fig. 6). Accuracy of ESI-Orbitrap-MS for the 44 fragment is 2.1‰ and for the C-1 position is 3.8‰, with $<1.5\text{‰}$ precision. Results shown here for ESI-Orbitrap-MS agree well with expected values from gas source IRMS instrumentation confirming that no recombination appears to be happening with ESI-Orbitrap-MS analyses. The agreement between ESI-Orbitrap-IRMS and GC-IRMS-based methods also confirms that the C-1 position of alanine is lost during fragmentation and the 44 fragment contains the C-2 and C-3 carbons.

3.1. An outlier

Two standards have the same MA values, C-1d and C-2c (Table 2). When the C-1 position liberated by ninhydrin was measured by GC-IRMS at Tokyo Tech, the two standards have different values: 10.3‰ and 0.3‰ respectively (Table 2). However, when both standards were (later) measured by ESI-Orbitrap-MS at Caltech, the values for the C-1 position were similar: -1.2‰ and -3.2‰ respectively (Table 2). The ESI-Orbitrap-MS values suggest that both standards that arrived at Caltech were likely to be aliquots of C-2c, possibly due to a labeling error. Therefore C-1d and C-2c are noted in red diamonds in Fig. 6. Both standards cannot be distinguished based solely on MA values, but their position-specific values allow them to be differentiated which made detecting the mislabeling possible.

3.2. ESI-Orbitrap-MS

ESI-Orbitrap-MS measurements are rapid (15 min) and highly sensitive, requiring 3–15 nmol of analyte per acquisition depending upon the type of information (molecular average or position-specific) desired. Triplicate analyses of standard brackets to constrain the molecular average, C-1, and residual positions can be done in about 4 h with only ~ 60 nmol of analyte. The sensitivity reported here (and in other ESI-Orbitrap-MS studies) for alanine is within the same order of magnitude required for GC-IRMS methods for amino acids (e.g., Ref. [33]).

It is hypothesized that all amino acids lose their C-1 position when

ionized by electrospray ionization followed by fragmentation in the HCD cell of an Orbitrap mass spectrometer [27]. Alanine is one of the smallest amino acids, and the loss of the C-1 position results in a fragment below the default mass cutoff of 50 m/z. Here we used service mode and additional tuning of ion optics parameters to access the mass range between 30 and 50 m/z and were able to detect the fragment representing the loss of the C-1 position in sufficient abundance to perform isotope ratio analysis. The C-2 and C-3 positions cannot be separated using the present method; however, it is possible that fragment ions containing these positions are generated within the HCD cell, but the resulting ions are below the lower limit of 30 m/z.

Because our results are accurate and were calculated assuming no rearrangement of atomic positions during the measurement, we conclude that no significant rearrangement occurs. Some of the molecular ion remains intact when fragmenting in the HCD cell, but this does not appear to alter the isotope ratios. The ESI-Orbitrap-MS methods presented here can easily be extended to other compounds where the corresponding positions between fragment and whole molecule are known. The main requirements are that the molecule is purified from a matrix so that no other compounds with similar m/z overlap (e.g., for reasons described in Ref. [34] and that it can be ionized by electrospray ionization. The ESI-Orbitrap-MS methods do not require derivatization and these systems can be interfaced with an HPLC for online separation prior to isotope analysis or using flow injections methods like those discussed by Ref. [23].

3.3. Relative merits and different uses of ESI and GC methods for PSIA

The ninhydrin/GC-based method allowed comparison of Orbitrap-based PSIA with IRMS-based PSIA. In the present study, 4.5 mg of each alanine standard was used to perform the ninhydrin reaction followed by isotope analyses by IRMS (compared to starting amount of 0.45 mg for ESI-Orbitrap-MS stock solutions). The GC methods are more time consuming, requiring 2 h for the initial ninhydrin reaction, 15 min for triplicate CO_2 analysis, 70 min for measuring $\delta^{13}\text{C}_{\text{MA}}$ of acetaldehyde three times, around 100 min to perform three GC-Py-GC-C-IRMS analyses of acetaldehyde and multiple 5–10 min SPME infusions and GC oven cooling, a total of >6 h per measurement. In addition, if the MA and PSIA acetaldehyde measurement were applied to a mixture of two or more amino acids, the ninhydrin reaction would constrain the average $\delta^{13}\text{C}$ value of CO_2 generated from the C-1 position of all amino acids combined. However, subsequent GC-Py-GC-IRMS analysis could separate the carbon positions of the individual aldehydes (data not shown), which would provide constraints of the differences between the C-2 and C-3 positions which is not presently possible using the ESI-Orbitrap-MS methods discussed here. The ninhydrin/GC method yields precise and accurate data on pure alanine, making it an excellent tool for study of small numbers of pure samples, and could be an appropriate approach to calibrating standards for ESI-Orbitrap-MS.

The ESI-Orbitrap-MS method discussed here can be compared to a similar technique, GC-Orbitrap-MS, which has been used to measure position-specific carbon isotope compositions of alanine from the Murchison meteorite [18]. The method requires derivatization, followed by GC-Orbitrap-MS analysis for MA and two fragments – one containing the C-2 and C-3 positions and the other containing the C-1 and C-2 positions. Using these three measurements, the carbon isotope composition of each of the carbon positions can be determined. GC-Orbitrap-MS analyses are useful for target analytes that are in low abundance (and amenable to derivatization) because of the online separation capabilities. However, at the time of writing, GC-Orbitrap-MS systems are only available in a few laboratories around the world. Published GC-Orbitrap methods can require many 2-h-long GC runs to achieve sample-standard comparison of several fragments (in some cases taking >24 h per sample). In contrast, ESI-Orbitrap-MS instruments have been widely used for proteomics and metabolomics research, so these tools are already available at many institutions. Infusion-based ESI-Orbitrap-MS has the

benefit of not requiring derivatization, but offline separation may be required for complex mixtures. ESI is a softer ionization; this has the advantage of limiting intramolecular recombination, but the disadvantage of not breaking the bond between the C-2 and C-3 positions. The methods discussed above, and the previously published ESI-Orbitrap-MS methods, used pure compounds and/or offline separation techniques. ESI-Orbitrap-MS instruments are easily coupled to HPLC systems which would permit online separation, albeit the measurement of high-precision isotope ratios in dynamic peaks has not yet been demonstrated by ESI-Orbitrap-MS. Even without online separation, the ESI-Orbitrap-MS instrumentation is amenable to high-throughput pipelines using separate methods for purification of underivatized amino acids by HPLC (e.g. Refs. [33,35,36]), followed by sequential introduction into the Orbitrap. Both Orbitrap-MS methods are viable for many compounds, and the choice of method will depend on the compound of interest and instrument availability.

3.4. Recommendations for PSIA by ESI-Orbitrap-MS

Analysis of ^{13}C -enriched alanine by ESI-Orbitrap-MS allowed for determination of some common issues and best practices for this method. We note that M+1 analysis results in a loss of intensity for the generated fragments, because M+1 analyses sample rare isotopologues which have <5% of the abundance of the unsubstituted ion and because the fragment at 44 m/z occurred outside of the Orbitrap's optimum mass range. Due to the low intensity, we used a lower AGC Target for the M+1 analysis, to reach the target number of ions more rapidly. This is of particular importance for the future investigation of PSIA by ESI-Orbitrap-MS for natural samples. To ensure that fragment ions are in sufficient abundance to be resolved from background ions, we recommend a starting concentration of at least 50 μM for the target analyte(s).

Once the ionization parameters have been optimized, maintaining stable signals and consistency between sample and standard with respect to both concentration of analytes and presence, type, and abundance of non-analyte ions is of great importance. It is best to keep the variation in NL score (i.e., ion intensity) across samples and standards to within 10% of each other. We found that analyses conducted during a single day that had >10% variation in the total ion current did not yield replicable isotope ratios. It is essential to ensure that sample and standard are analyzed under as close to the same parameters as possible, especially if contaminant (i.e., non-analyte) co-eluting peaks are present. Previous studies have noted that presence of contaminant ions can suppress the ^{13}C -substituted signal (e.g., Ref. [34]). Mass selection in the AQT quadrupole prior to Orbitrap analysis can often remove contaminants. And, in some cases, the HCD cell can be used to remove contaminant peaks with no effect on analyte peaks.

For the analyses presented here, we settled on a few best practices. First, we initially chose to use three standard replicates to bracket our ^{13}C -enriched standard analyses in triplicate to account for variation between acquisitions when analyzing molecular average values. Natural abundance standard – ^{13}C -enriched standard – natural abundance standard bracketing gives similar results (e.g. Ref. [23]), and was used for the 44 fragment measurements. We recommend bracketing single sample analyses with standards of known isotopic composition rather than analyzing multiple, different samples in between standard brackets. At the time of writing, off-line characterized standards are being used. We also note that, in contrast to EA-IRMS, the standards used must be the same as target analytes, which might be limiting if a large variety of compounds are being measured. Second, rinsing the syringe and tubing with pure methanol between analyses caused residual analyte in the system to be <5% of the analyte abundance for alanine. It is important to determine this for the target analyte before deciding if blank subtraction or additional solvent rinses are necessary. Third, when linking ESI-Orbitrap-MS values to the VPDB scale, we note a larger offset for standards with more ^{13}C -enriched values (Fig. S3). We used only one standard with a narrow range of position-specific values (in VPDB space)

between –13 and –7‰. An additional bracketing standard of known composition with more ^{13}C -enriched values at individual atomic positions is necessary to accurately calibrate samples with more ^{13}C -enrichment relative to VPDB.

Other methods (e.g., GC-Py-GC-C-IRMS, GC-Orbitrap-MS, nuclear magnetic resonance spectroscopy) come with their own set of challenges and in many scenarios ESI-Orbitrap-MS is a more feasible option for measuring the position-specific isotope composition of small organic molecules. A large variety of compounds are amenable to ESI-Orbitrap-MS analysis and the instrumentation is already being widely used in laboratories around the world. Software for making high-precision, natural abundance isotope measurements (i.e., IsoX) is not standard, but currently in development for distribution by Thermo Fisher Scientific. Fragmentation mechanisms are well-studied, as they are a part of routine compound identification methods, and ESI-Orbitrap-MS instruments are easily coupled to an HPLC for online separation. For these reasons, we anticipate that isotope analysis by ESI-Orbitrap-MS will be a rapidly expanding area of research over the next decade, particularly for biomolecules.

4. Summary and conclusions

Here we demonstrate the utility and accuracy of ESI-Orbitrap-MS instrumentation for molecular average and position-specific carbon isotope analysis of alanine. Using ^{13}C -labeled standards of known isotopic composition, we show that ESI-Orbitrap-MS methods confidently recover the isotopic enrichment at the full molecule, C-1 position, and average C-2 + C-3 positions. These results confirm the lack of recombination for ESI-Orbitrap-MS analyses and demonstrate that the C-1 position is lost during fragmentation. Precision and accuracy for molecular average measurements was $\leq 1\%$. Precision for ESI-Orbitrap-MS measurements of the 44 fragment was 2.1‰ and for the C-1 calculations, precision was 3.8‰. Accuracy was <1.5‰ for both measurements. Importantly, the method presented above can be adapted to constrain the carbon isotope composition of the C-1 position for all amino acids and other small organics with known fragmentation patterns (e.g., Refs. [14,27]). ESI-Orbitrap-MS is a robust tool that permits accurate quantification of isotopic differences on biologically relevant scales and provides a way of determining position-specific isotope information without the need for derivatization or chemical degradation. This new approach to measuring isotope ratios could be particularly useful for compounds that do not derivatize well or tend to yield incomplete combustion products and are therefore not amenable to GC-IRMS based systems.

Data and materials availability

Data, including, RAW files generated by the instrument and, txt files generated by FTStatistic, is available on the Caltech data repository (<https://doi.org/10.22002/xz4cp-hyd02>). Code for our data processing is available at github.com/Csernica/Alanine_M1 and stored on the open Zenodo repository (<https://zenodo.org/record/7963550>).

Declaration of competing interest

All authors declare that there are no conflicts of interest with the work presented in the manuscript “Analysis of intramolecular carbon isotope distributions in alanine by electrospray ionization Orbitrap mass spectrometry.”

Data availability

Data has been uploaded to online repositories and the links are included in the main text.

Acknowledgments

This work was supported by a NASA Astrobiology Institute (grant number 80NSSC18M094) and DOE-BES support to JME. MJ also thanks the JSPS (no P17725) for funding his postdoctoral fellowship. All members of the Orbitrap subgroups at Caltech and Penn State are thanked for helpful discussions encompassing all aspects of Orbitrap isotope ratio analysis and data processing. We greatly appreciate discussions with Caj. Neubauer during the method optimization stage. We would like to acknowledge Fenfang Wu and Makalya Betts for their help with EA-IRMS analyses at Caltech.

Appendix A. Supplementary data

Supplementary data to this article can be found online at <https://doi.org/10.1016/j.ijms.2023.117128>.

References

- J.M. Hayes, Fractionation of carbon and hydrogen isotopes in biosynthetic processes, *Rev. Mineral. Geochem.* 43 (2001) 225–277, <https://doi.org/10.2138/gsrmg.43.1.225>.
- P.H. Abelson, T.C. Hoering, Carbon isotope fractionation in formation of amino acids by photosynthetic organisms, *Proc. Natl. Acad. Sci. USA* 47 (1961) 623–632, <https://doi.org/10.1073/pnas.47.5.623>.
- K.D. Monson, J.M. Hayes, Biosynthetic control of the natural abundance of carbon-13 at specific positions within fatty acids in *Escherichia coli*. Evidence regarding the coupling of fatty acid and phospholipid synthesis, *J. Biol. Chem.* 255 (1980) 11435–11441, [https://doi.org/10.1016/S0021-9258\(19\)70310-X](https://doi.org/10.1016/S0021-9258(19)70310-X).
- A. Rossmann, M. Butzenlechner, H.-L. Schmidt, Evidence for a nonstatistical carbon isotope distribution in natural glucose, *Plant Physiology* 96 (1991) 609–614, <https://doi.org/10.1104/pp.96.2.609>.
- T.N. Corso, J.T. Brenna, High-precision position-specific isotope analysis, *Proceedings of the National Academy of Sciences USA* 94 (1997) 1049–1053, <https://doi.org/10.1073/pnas.94.4.1049>.
- G.L. Sacks, J.T. Brenna, High-precision position-specific isotope analysis of $^{13}\text{C}/^{12}\text{C}$ in leucine and methionine analogues, *Anal. Chem.* 75 (2003) 5495–5503.
- A. Gilbert, K. Yamada, K. Suda, Y. Ueno, N. Yoshida, Measurement of position-specific ^{13}C isotopic composition of propane at the nanomole level, *Geochem. Cosmochim. Acta* 177 (2016) 205–216, <https://doi.org/10.1016/j.gca.2016.01.017>.
- R.F. Dias, K.H. Freeman, S.G. Franks, Gas chromatography-pyrolysis-isotope ratio mass spectrometry: a new method for investigating intramolecular isotopic variation in low molecular weight organic acids, *Org. Geochem.* 22 (2020) 161–168.
- T. Jézéquel, V. Joubert, P. Giraudeau, G.S. Remaud, S. Akoka, The new face of isotopic NMR at natural abundance, *Magn. Reson. Chem.* 55 (2017) 77–90, <https://doi.org/10.1002/mrc.4548>.
- S. Akoka, G.S. Remaud, NMR-based isotopic and isotopomic analysis, *Prog. Nucl. Magn. Reson. Spectrosc.* 120–121 (2020) 1–24, <https://doi.org/10.1016/j.pnmrs.2020.07.001>.
- G.J. Martin, M.L. Martin, Deuterium labelling at the natural abundance level as studied by high field quantitative ^2H NMR, *Tetrahedron Lett.* 22 (1981), [https://doi.org/10.1016/S0040-4039\(01\)81948-1](https://doi.org/10.1016/S0040-4039(01)81948-1), 3525–2538.
- D.W. Hoffman, C. Rasmussen, Position-specific carbon stable isotope ratios by proton NMR spectroscopy, *Analytical Chem.* 91 (2020) 15661–15669, <https://doi.org/10.1021/acs.analchem.9b03776>.
- J. Eiler, J. Cesar, L. Chimiak, B. Dallas, K. Grice, J. Griep-Raming, D. Juchelka, N. Kitchen, M. Lloyd, A. Makarov, R. Robins, J. Schweiters, Analysis of molecular isotopic structures at high precision and accuracy by Orbitrap mass spectrometry, *Int. J. Mass Spectrom.* 422 (2017) 126–142, <https://doi.org/10.1016/j.ijms.2017.10.002>.
- C. Neubauer, M.J. Sweredoski, A. Moradian, D.K. Newman, R.J. Robins, J.M. Eiler, Scanning the isotopic structure of molecules by tandem mass spectrometry, *Int. J. Mass Spectrom.* 434 (2018) 276–286, <https://doi.org/10.1016/j.ijms.2018.08.001>.
- J.M. Eiler, M. Clog, P. Magyar, A. Piasecki, A. Sessions, D. Stolper, M. Deerberg, H.-J. Schlueter, J. Schwieters, A high-resolution gas-source isotope ratio mass spectrometer, *Int. J. Mass Spectrom.* 335 (2013) 45–56, <https://doi.org/10.1016/j.ijms.2012.10.014>.
- E.P. Mueller, A.L. Sessions, P.E. Sauer, G.M. Weiss, J.M. Eiler, Simultaneous, high-precision measurements of $\delta^2\text{H}$ and $\delta^{13}\text{C}$ in nanomole quantities of acetate using electrospray ionization-quadrupole-Orbitrap mass spectrometry, *Anal. Chem.* 94 (2022) 1092–1100, <https://doi.org/10.1021/acs.analchem.1c04141>.
- J. Cesar, J. Eiler, B. Dallas, L. Chimiak, K. Grice, Isotope heterogeneity in ethyltoluenes from Australian condensates, and their stable carbon site-specific isotope analysis, *Org. Geochem.* 135 (2019) 32–37, <https://doi.org/10.1016/j.orggeochem.2019.06.002>.
- L. Chimiak, J.E. Elsil, B. Dallas, J.P. Dworkin, J.C. Aponte, A.L. Sessions, J. M. Eiler, Carbon isotope evidence for the substrates and mechanisms of probiotic synthesis in the early solar system, *Geochem. Cosmochim. Acta* 292 (2021) 188–202, <https://doi.org/10.1016/j.gca.2020.09.026>.
- E.B. Wilkes, A.L. Sessions, S.S. Zeichner, B. Dallas, B. Schubert, A. Hope Jahren, J. M. Eiler, Position-specific carbon isotope analysis of serine by gas chromatography/Orbitrap mass spectrometry, and an application to plant metabolism, *Rapid Commun. Mass Spectrom.* 36 (2022) e9347, <https://doi.org/10.1002/rcm.9347>.
- S.Z. Zeichner, E.B. Wilkes, A.E. Hofmann, L. Chimiak, A.L. Sessions, A. Makarov, J. M. Eiler, Methods and limitations of stable isotope measurements via direct elution of chromatographic peaks using gas chromatography-Orbitrap mass spectrometry, *Int. J. Mass Spectrom.* 477 (2022), 116848, <https://doi.org/10.1016/j.ijms.2022.116848>.
- M. Scigelova, A. Makarov, Orbitrap mass analyzer – overview and applications in proteomics, *Proteomics* 6 (2006) 16–21, <https://doi.org/10.1002/pmic.200600528>.
- C. Neubauer, A. Crémère, X.T. Wang, N. Thiagarajan, A.L. Sessions, J.F. Adkins, N. F. Dalleska, A.V. Turchyn, J.A. Clegg, A. Moradian, M.J. Sweredoski, S.D. Garbis, J. M. Eiler, Stable isotope analysis of intact oxanions using electrospray quadrupole-Orbitrap mass spectrometry, *Anal. Chem.* 93 (2020) 3077–3085, <https://doi.org/10.1021/acs.analchem.9b04486>.
- A. Hilkert, J.K. Böhlke, S.J. Mroczkowski, K.L. Fort, K. Aizikov, X.T. Wang, S. H. Kopf, C. Neubauer, Exploring the potential of electrospray-Orbitrap for stable isotope analysis using nitrate as a model, *Anal. Chem.* 93 (2021) 9139–9148, <https://doi.org/10.1021/acs.analchem.1c00944>.
- L. Chimiak, J. Eiler, A. Sessions, C. Blumenfeld, M. Klatte, B.M. Stoltz, Isotope effects at the origin of life: fingerprints of the Strecker synthesis, *Geochem. Cosmochim. Acta* 321 (2022) 78–98, <https://doi.org/10.1016/j.gca.2022.01.015>.
- S. Pizzarello, R.V. Krishnamurthy, S. Epstein, J.R. Cronin, Isotopic analyses of amino acids from the Murchison meteorite, *Geochem. Cosmochim. Acta* 55 (1991) 905–910, [https://doi.org/10.1016/0016-7037\(91\)90350-E](https://doi.org/10.1016/0016-7037(91)90350-E).
- J.E. Elsil, S.B. Charnley, A.S. Burton, D.P. Glavin, J.P. Dworkin, Compound-specific carbon, nitrogen, and hydrogen isotopic ratios for amino acids in CM and CR chondrites and their use in evaluating potential formation pathways: amino acid stable isotopes and formation pathways, *Meteoritics Planet. Sci.* 47 (2012) 1517–1536, <https://doi.org/10.1111/j.1945-5100.2012.01415.x>.
- P. Zhang, W. Chan, I.L. Ang, R. Wei, M.M.T. Lam, K.M.K. Kei, T.C.W. Poon, Revisiting fragmentation reactions of protonated α -amino acids by high-resolution electrospray ionization tandem mass spectrometry with collision-induced dissociation, *Sci. Rep.* 9 (2019) 6453, <https://doi.org/10.1038/s41598-019-42777-8>.
- B. Fry, J.F. Carter, K. Yamada, N. Yoshida, D. Juchelka, Position-specific $^{13}\text{C}/^{12}\text{C}$ analysis of amino acid carboxyl groups – automated flow-injection analysis based on reaction with ninhydrin, *Rapid Commun. Mass Spectrom.* 32 (2018) 992–1000, <https://doi.org/10.1002/rcm.8126>.
- T.N. Corso, J.T. Brenna, On-line pyrolysis of hydrocarbons coupled to high-precision carbon isotope analysis, *Anal. Chim. Acta* 397 (1999) 217–224, [https://doi.org/10.1016/S0003-2670\(99\)00406-7](https://doi.org/10.1016/S0003-2670(99)00406-7).
- M. Julien, M.J. Goldman, C. Liu, J. Horita, C.J. Boreham, K. Yamada, W.H. Green, N. Yoshida, A. Gilbert, Intramolecular ^{13}C isotope distributions of butane from natural gases, *Chem. Geol.* 541 (2020), 119571, <https://doi.org/10.1016/j.chemgeo.2020.119571>.
- A. Makarov, E. Denisov, Dynamics of ions of intact proteins in the Orbitrap mass analyzer, *Journal of the American Association of Mass Spectrometry* 20 (2009) 1486–1495, <https://doi.org/10.1016/j.jasms.2009.03.024>.
- T. Csernica, J.M. Eiler, High-dimensional isotomics, part 1: a mathematical framework for isotomics, *Chem. Geol.* 617 (2023), 121235, <https://doi.org/10.1016/j.chemgeo.2022.121235>.
- S.N. Silverman, A.A. Phillips, G.M. Weiss, E.B. Wilkes, J.M. Eiler, A.L. Sessions, Practical considerations for amino acid isotope analysis, *Org. Geochem.* 164 (2022), 104345, <https://doi.org/10.1016/j.orggeochem.2021.104345>.
- A.E. Hofmann, L. Chimiak, B. Dallas, J. Griep-Raming, D. Juchelka, A. Makarov, J. Schwieters, J.M. Eiler, Using Orbitrap mass spectrometry to assess the isotopic compositions of individual compounds in mixtures, *Int. J. Mass Spectrom.* 457 (2020), 11310, <https://doi.org/10.1016/j.ijms.2020.116410>.
- J.A. Tripp, J.S. McCullagh, R.E. Hedges, Preparative separation of underivatized amino acids for compound-specific stable isotope analysis and radiocarbon dating of hydrolyzed bone collagen, *J. Separ. Sci.* 29 (2006) 41–48, <https://doi.org/10.1002/jssc.200500247>.
- Y. Sun, N.F. Ishikawa, N.O. Ogawa, H. Kawahata, Y. Takano, N. Ohkouchi, A method for stable carbon isotope measurement of underivatized amino acids by multi-dimensional high-performance liquid chromatography and elemental analyzer/isotope ratio mass spectrometry, *Rapid Commun. Mass Spectrom.* 34 (2020), e8885, <https://doi.org/10.1002/rcm.8885>.